

Re-elucidation of the acid-catalyzed urea-formaldehyde reactions: A theoretical and ^{13}C -NMR study

Taohong Li,¹ Jiankun Liang,^{1,2} Ming Cao,^{1,2} Xiaoshen Guo,¹ Xiaoguang Xie,³ Guanben Du¹

¹The Key Laboratory of Wood Adhesives and Glued Products of Yunnan Province, Southwest Forestry University, Kunming 650224, People's Republic of China

²Beijing Forestry University, Beijing 100000, People's Republic of China

³Department of Chemistry, Yunnan University, Kunming 650091, People's Republic of China

Correspondence to: G. Du (E-mail: dgb510@163.com)

ABSTRACT: The acid-catalyzed urea-formaldehyde reactions were reexamined in detail by using quantum chemistry method and ^{13}C -NMR determinations. Some issues in the synthesis theory that were not well understood previously have been addressed and clarified. The identified reaction mechanisms and calculated energy barriers suggest that the competitive formations of methylene and methylene ether linkages are kinetically affected by both reaction energy barriers and steric hindrance effect. The thermodynamic properties determine that the methylene linkages are dominant at the late condensation stage. The theoretical results well rationalized the observed different changing processes of resin structures with different F/U molar ratios. The previously proposed mechanism for transformation of methylene ether linkage to methylene linkage cannot explain the structural changes during condensation, and thus, other mechanisms were proposed. The calculated results for uron explained the fact that the formation of such structure is much slower than other structures under weak acidic condition. © 2016 Wiley Periodicals, Inc. *J. Appl. Polym. Sci.* **2016**, *133*, 44339.

KEYWORDS: adhesives; catalysts; resins; structure-property relationship; theory and modeling

Received 8 May 2016; accepted 5 August 2016

DOI: [10.1002/app.44339](https://doi.org/10.1002/app.44339)

INTRODUCTION

Urea-formaldehyde (UF) resin is the currently most widely used adhesives in modern wood industry. The good binding strength and low cost are the main reasons for its wide applications. However, the shortcomings of this resin are also distinct, like the formaldehyde emission and poor water resistance. The root of the formaldehyde emission lies in the reversibility of the addition and condensation reactions, whereas the poor water resistance is mainly due to the low stability of the chemical bonds in the polymers toward hydrolysis.^{1,2} So far, the best strategy to solve the first problem is to lower the formaldehyde/urea (F/U) molar ratio by adding additional urea at the final alkaline reaction stage. This strategy can not only significantly lower the formaldehyde emission level but also partly sacrifices the binding strength. The water resistance performance may be improved by introducing the third and even the fourth reactant as the new components of the resin. These resins are called modified UF resins. For example, by introducing melamine into the UF system, the water resistance ability may be improved to some extent.³⁻¹⁰ It is believed that the co-condensations of the newly introduced components with UF would produce better resins because a certain good property of the components may be grafted on UF resin.

A better understanding of the reaction mechanisms is the prerequisite of taking any strategy to improve the performance of the resin. The fundamental theory established through reaction kinetics studies in the middle of the last century provided the basic information of the addition and condensation reactions in urea-formaldehyde system.¹⁰⁻¹⁴ However, such fundamental theory appears to be incapable of describing the very complicated formation processes of UF polymer structures because a number of competitive reactions are involved and the components and structures of the polymers are sensitive to the changes of reaction conditions like molar ratio, pH, temperature, and so forth. To further understand the influences of the reaction conditions on the polymers, numerous studies which used analytic techniques, like NMR, MS, and IR, are carried out during the past decades.¹⁵⁻²⁹ These studies have indeed provided many useful details about the structures of the polymers. However, they provided limited information about how the structures are formed and why they are different with respect to different conditions.

After studying a number of literatures published during the past decades,¹⁻²⁹ we found that some fundamental but important issues regarding the theory of UF resin synthesis have not been

clarified and some concepts which seem reasonable and have been widely accepted need to be reexamined. Many experiments indicate that the base-catalyzed polymerizations of methylolureas mainly produce methylene ether linkages ($-\text{NR}-\text{CH}_2-\text{O}-\text{CH}_2-\text{NR}-$), whereas the more stable and branched methylene linkages ($-\text{NR}-\text{CH}_2-\text{NR}-$) cannot be formed. This is the right reason that the synthesis of UF resin must experience acidic stage. Our recent theoretical calculations and experiments have rationalized these experimental observations.³⁰ It was found that the higher reaction potential energy barrier and steric hindrance effect are the key factors that suppress the formation of methylene linkages. After canceling the steric hindrance, the formation of methylene linkages became much more competitive (see details in ref. 30). However, all the reported experiments clearly show that the methylene linkages can be formed dominantly in the acid-catalyzed reactions with F/U = 2/1 or higher molar ratio. How to understand the competitive relationship of the two linkages under acidic conditions? To the best of our knowledge, this issue has not been well addressed so far. Furthermore, the rearrangement of a portion of methylene ether linkages to methylene linkages can always be observed during acidic reaction, and the emission of free formaldehyde is also accompanied. After careful analysis of some ¹³C-NMR data, we found that simple splitting-off of a formaldehyde molecule from an ether linkage apparently cannot explain some changes of polymer structures during synthesis. What is the exact mechanism for the rearrangement? It was proposed that the uron structure can be formed through self-cyclization of methylolureas; however, the content is generally much lower than other structures under weak acidic condition.^{21–24,31–33} How to explain this result? These fundamental but important issues were clarified in the current work by theoretical calculations carried out on the acid-catalyzed elementary reactions of UF system. The calculated results and related inferences are supported by the designed experiments and ¹³C-NMR determinations.

QUANTUM CHEMISTRY CALCULATIONS AND EXPERIMENTS

Quantum Chemistry Calculations

All the geometries of the stationary points on the reaction potential energy surfaces (PES), including reactants, intermediates, transition states and products, were fully optimized by using MP2 (ref. 34) method with the standard basis set 6-31++G**.³⁵ The harmonic vibrational frequencies were calculated to characterize the nature of the stationary points and to obtain the zero-point energies (ZPE) which were used to correct the relative energies. Each transition state was identified as it has unique imaginary frequency. For all the calculations, the self-consistent reaction field method was used with polarizable continuum model^{35–37} by defining water as the solvent to simulate the implicit solvent effects (water: $\epsilon = 78.3553$). All the calculations were carried out with GAUSSIAN 03 program package.³⁸

Sample Preparations

The analytical reagent (AR)-grade urea, sodium hydroxide, and formaldehyde (37%, w/w) containing about 7% methanol were bought from the market (Sinopharm Chemical Reagent Co., Ltd.). The formaldehyde solution was initially brought to pH of about 5.5–6.0 (measured with a pH meter) at room temperature using 20% NaOH. Then, 11.1 g and 22.2 g urea (U) were mixed

with 30.0 g formaldehyde solution, respectively, to obtain the F/U molar ratio of 2/1 and 1/1. After the urea dissolved completely, the pHs of the mixtures were tested and readjusted to 5.5–6.0. The mixtures were then charged into a three-necked flask equipped with a reflux condenser, mechanical stirrer, and thermometer. Each mixture was heated to 75 °C in water bath. The mixture with molar ratio of 2/1 was allowed to react for 4 h, and for every 1 h, one sample was taken, and the four samples were denoted as UFA-1, UFA-2, UFA-3, and UFA-4, respectively. For the 1/1 mixture, the total reaction time was 1 h. Two samples were taken at 0.5 h and 1 h, and they are denoted as UFB-1 and UFB-2, respectively. After the mixtures were cooled down, the ¹³C-NMR determinations were carried out.

Procedure for ¹³C-NMR Spectra

About 400 μL liquid sample was directly mixed with 50 μL of DMSO-*d*₆ for ¹³C-NMR determinations of UFA-1–UFA-4. Because of the fact that the samples UFB-1 and UFB-2 are somewhat cloudy, 300 μL liquid sample was mixed with 150 μL DMSO-*d*₆ to make sure that all components are dissolved. The spectra were obtained on a Bruker-AVANCE 600 NMR spectrometer using 12- μs pulse width (90°). A 6-s relaxation delay was used to secure quantitative results of methylenic carbons which showed *T*₁ values of 0.16 s or smaller by the inversion-recovery method.²¹ To achieve a sufficient signal-to-noise ratio, inverse-gated proton decoupling method was applied. The spectra were taken at 150 MHz with 400–600 scans accumulated. The observed chemical shifts were assigned by referring to the assignments in the literatures.^{19–24}

From the obtained spectral peak integration values, the methylenic carbons and urea carbonyls were separately summed, and the various carbon groups were calculated into percentages, or defined as molar percentages. Specifically, the molar distribution of the structural elements was described by the percentages calculated from the following formula:

$$\text{Molar \%} = \frac{A_i}{\sum_i A_i} \times 100 \%$$

Here, the *A_i* is the integration value of an individual peak area and the denominator is the sum of the integration values for all the peaks of methylenic carbons or urea carbonyl carbons. As all the methylenic carbons are from different forms of formaldehyde and all the carbonyl carbons are from urea, the obtained percentages can be defined as molar percentages of formaldehyde and urea, respectively.

As the *T*₁ measured for different urea carbonyls are 1.4–6.2 s,²¹ the 6-s relaxation delay may not long enough to assure satisfactory integration results. Therefore, these results are only used to assist the main discussions on quantitative results of methylenic carbons.

RESULTS AND DISCUSSION

Mechanisms of Methylation

Before discussion, it should be claimed that all the potential energy barriers calculated in this study for the involved reactions are those for elementary reactions, and these barriers are not equivalent to the experimentally measured apparent activation energies,

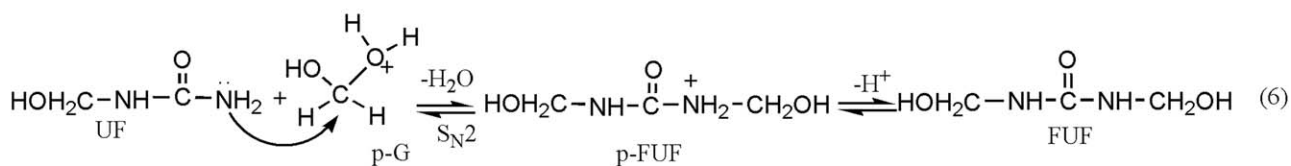
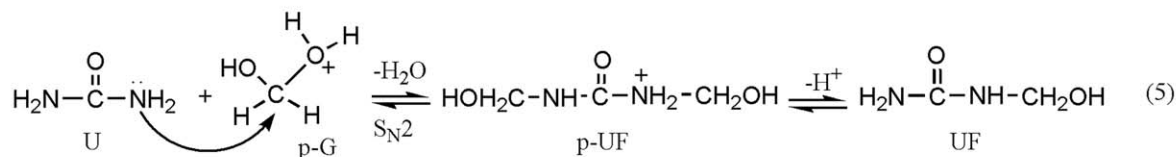
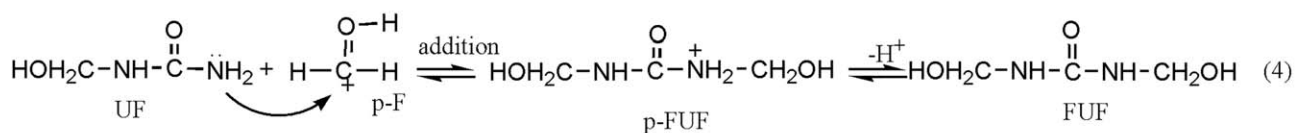
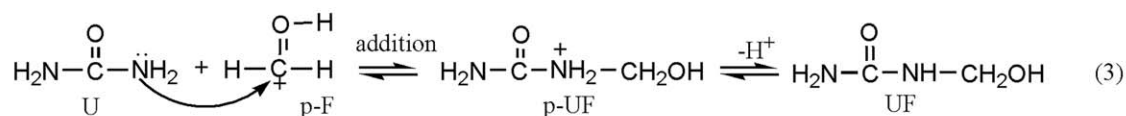
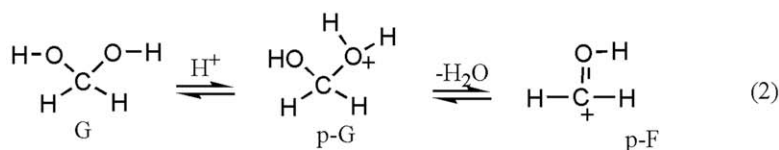
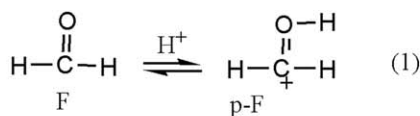


Figure 1. The mechanisms for acid-catalyzed methylation of urea.

which are the overall results for many simultaneous reactions. The calculated energy barriers here are used to estimate the relative rates of different elementary reactions or reaction steps.

The early kinetic studies have pointed out that the protonated formaldehyde is highly reactive species toward nucleophiles like urea.^{10,38} This is the right reason that the methylation of urea under acidic condition is much faster than that in neutral or alkaline solution. However, in water solution, formaldehyde exists mainly in the form of methanediol, which can also be protonated and participate in methylation reactions. The reactions (1)–(6) in Figure 1 show that the mechanisms of the reactions of urea and monomethylol urea with the protonated formaldehyde and methanediol. In the current study, the nucleophilic attack step (the first step) of the reactions (3)–(6) was theoretically studied. Considering that the protonation and deprotonation are generally fast reactions in solution, the second step of these reactions were not calculated.

The calculated results shown in Figure 2 demonstrate the potential energy profiles and the structures of the intermediates, transition states, and products. In the reaction of urea with protonated formaldehyde, the stable hydrogen-bonding complex

U-pF can be initially formed. This complex is lower in energy than the starting reactants (U + pF) by 101.3 kJ/mol. The short hydrogen bond (0.1622 nm) agrees with this large bonding energy. It is apparent that the proton is more likely located on the carbonyl oxygen of urea instead of formaldehyde, indicating that this complex may be originated from protonated urea and free formaldehyde. However, the proton is obviously on the oxygen atom of formaldehyde in the transition state TS-U-pF. To clarify this issue, the intrinsic reaction coordinate calculation was performed. The result showed that the proton is indeed initially on the urea and gradually move to formaldehyde with the attacking of amino group on carbon atom of formaldehyde. Figure 3 shows two possible hydrogen-bonding complexes. We speculated that the complex A should be formed when protonated formaldehyde molecule collides with urea. However, geometry optimizations indicate such complex does not exist. Therefore, it is referred that proton transfer could occur to form complex B when protonated formaldehyde collides with urea. Once the nucleophilic attack begins, the proton shifts back to formaldehyde to form hydroxymethyl group. This indicates that the carbonyl oxygen of urea has higher proton affinity than that of formaldehyde. In this context, it should be safe to

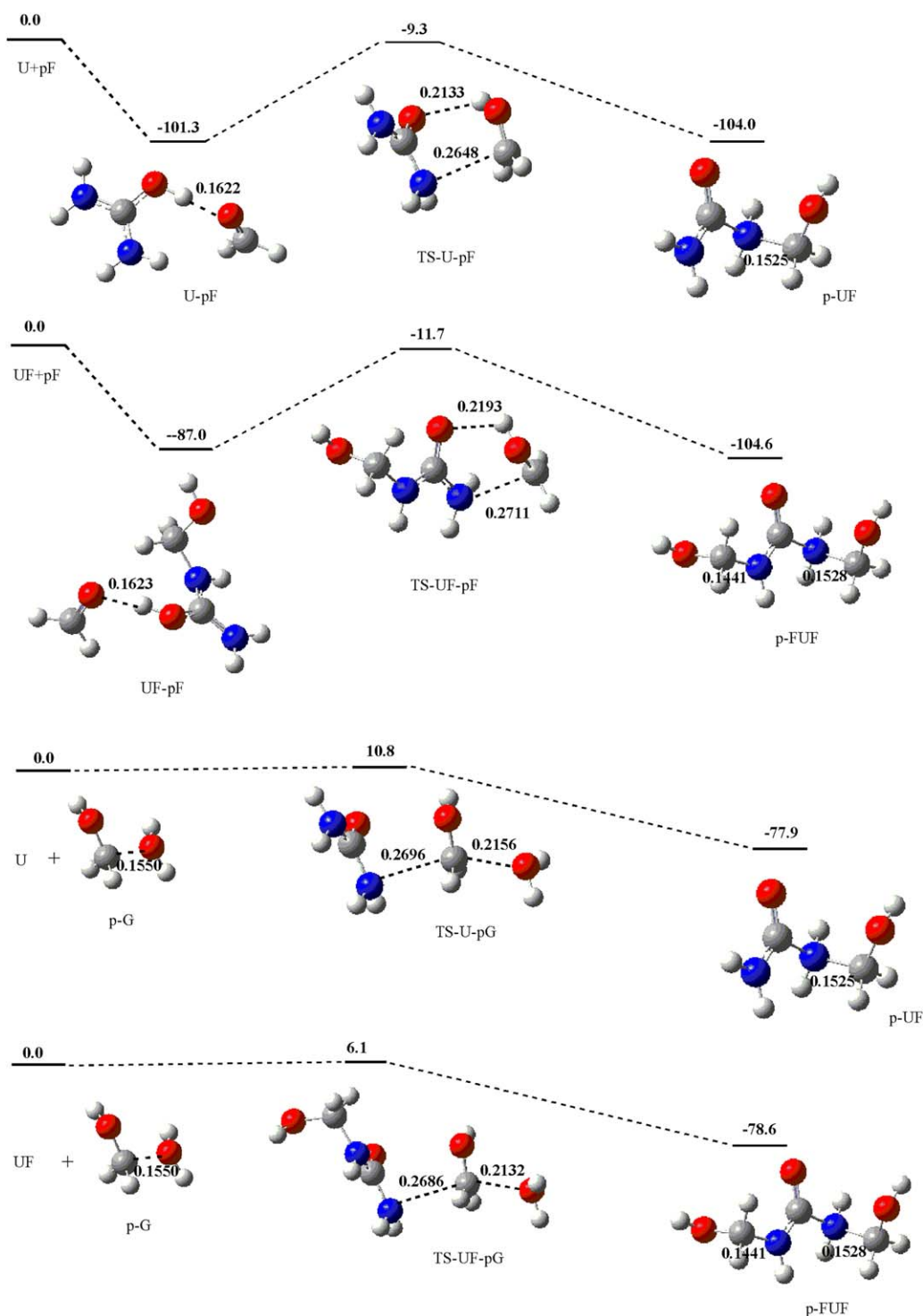


Figure 2. The structures (bond length in nm) and relative energies (kJ/mol) of the stationary points on PESs of reactions (3)–(6). [Color figure can be viewed at wileyonlinelibrary.com.]

conclude that both urea and formaldehyde can be protonated in acidic solution. Because of the remarkable stability of U-pF, the transition state TS-U-pF has notable barrier of 92.0 kJ/mol. After TS-U-pF, the product p-UF can be formed, and it is more stable than the initial reactants by 104.0 kJ/mol. Deprotonation of p-UF produces neutral monomethylol urea. Further reaction

between monomethylol urea and formaldehyde produces *N,N'*-dimethylolurea. As shown in Figure 2, in this reaction, the transition state TS-UF-pF has barrier of 75.3 kJ/mol with respect to the hydrogen-bonding complex UF-pF. This lower barrier suggests that the reaction between monomethylolurea and formaldehyde is faster than the reaction of urea with formaldehyde.

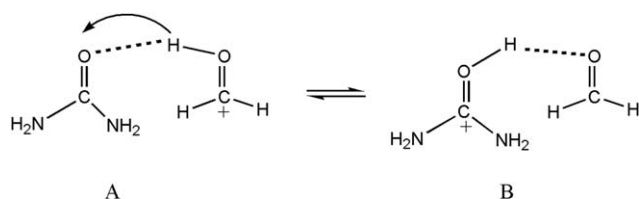


Figure 3. Two possible complexes formed between protonated formaldehyde and urea.

As it can be seen in Figure 2, the reaction between urea and protonated methanediol undergoes through bimolecular nucleophilic substitution (S_N2) mechanism. Because of the protonation, one of the C—O bonds in methanediol is significantly weakened as it was calculated to be 0.1550 nm, which is much longer than a normal C—O bond (around 0.14 nm). As a result, the nucleophilic attack of urea on methanediol encounters a small energy barrier of 10.8 kJ/mol. Similar reaction occurs between monomethylol urea and protonated methanediol, and the barrier is slightly lower. Apparently, theoretical calculations suggest that the protonated methanediol is much more reactive than the protonated formaldehyde. In addition to the much higher concentration of methanediol than formaldehyde, we prefer that methanediol contributes mainly to the formation of methylolureas.

It should be noted that although theoretical calculations indicate that the reaction between urea and protonated methanediol would be very fast, the experimentally measured reaction rate would be much slower due to the fact that the concentration of the proton is much lower than the concentration of urea and formaldehyde (methanediol) no matter in weak or strong acidic condition. In other words, the protonated reactants are in very small portion. However, the rate is indeed dependent on the pH as the concentration of proton determines the concentration of reactive protonated intermediates.

Mechanisms of Condensation

With catalysis of acid, methylolureas can condensate to form polymers linked with methylene and methylene ether linkages. Two types of reaction mechanisms have been suggested and shown in Figure 4. In the earlier kinetics study in 1953 by De Jong *et al.*, the condensations of methylolureas exhibited biomolecular features,¹⁴ whereas Francis *et al.*³⁹ in 1983 inferred a different mechanism that concerns the formation of carbon cation intermediate that generally represents a unimolecular mechanism. Recently, Sun *et al.*³³ suggested again the biomolecular mechanism. The classical organic theory tells that some alcohols like ally alcohol and benzyl alcohol can produce carbon cation, which acts as active intermediates in substitution reactions, and the mechanism has been characterized to be unimolecular (S_N1). The favorable formation of carbon cation is mainly due to the p- π conjugation effect that efficiently distributes the positive charge in the intermediate. Similarly, for methylolurea, elimination of a water molecule from the protonated hydroxymethyl group will produce the carbon cation which can be stabilized by strong conjugation effect. Therefore, we prefer the unimolecular mechanism for the methylolurea condensations.

For the S_N1 reaction, the formation of carbon cation is generally the rate-determining step. In the current study, the production of carbon cation from methylolurea was investigated, and the proposed mechanisms are shown in Figure 5. After the formation of nitrogen-protonated methylolurea (N-p-UF), one of the protons can shift to hydroxymethyl group, forming the oxygen-protonated methylolurea (O-p-UF) from which a water molecule is eliminated to produce the carbon cation (CBC). Considering that the proton-transfer reaction in water solution may be catalyzed by water molecule, we proposed another reaction path where a water molecule mediates the proton transfer from nitrogen to oxygen. In CBC, the nitrogen atom can donate the lone-paired electrons to the electron-deficient carbon atom to form an N—C π bond. Through π - π conjugation, the delocalization of electrons can occur. In other words, the positive charge can be redistributed, and as a result, the cation is stabilized. In brief, the special electronic structure of the methylolurea carbon cation makes it similar with ally and benzyl alcohol carbon cation.

Figure 6 shows the theoretically calculated results for the CBC formation mechanisms. As it can be seen, direct transfer of a proton from nitrogen to oxygen can occur via the four-member ring transition state N-O-TS; however, a notable energy barrier of 123.8 kJ/mol is encountered in this step. This is not in agreement with the experimentally observed fast condensation reaction under acidic condition. With the mediation of a water molecule, the proton transfer barrier is significantly lowered to be 40.6 kJ/mol, and this is the highest barrier on the potential energy surface. The water dissociation transition state W-Diso-TS has small barrier of 24.8 kJ/mol relative to W-O-p-UF, indicating that the C—O bond is largely weakened by protonation and also reflecting the remarkable stability of CBC. However, it should be realized that the CBC is still a very active intermediate in comparison with normal molecule.

In the condensation reactions, the CBC reacts with methylolureas to form methylene or methylene ether linkages. Some representative condensation reactions are shown in Figure 7 as (7)–(10). The theoretically calculated results for reactions (7) and (8) are given in Figure 8. In the reaction of free urea (U) with CBC, the complex U-CBC is initially formed through weak hydrogen bonding. Through nucleophilic attack of $-\text{NH}_2$ group on $-\text{CH}_2$ group, the methylene linkage can be formed. The transition state of this step is U-CBC-TS which has small barrier of 8.1 kJ/mol relative to U-CBC, indicating that the reaction would be very fast. The formed product methylenediurea (MDU) is more stable than the reactants U + CBC by 60.9 kJ/mol. Because a proton is still on the nitrogen atom, this product is denoted as p-MDU. In contrast, the transition state UF-CB-TS corresponding to the formation methylene ether linkage has higher barrier of 38.2 kJ/mol with respect to the initially formed complex UF-CBC. This suggests that the reaction between CBC and a free $-\text{NH}_2$ group is energetically more favorable than the reaction between CBC and $-\text{OH}$ group.

In the kinetics study by De Jong *et al.*,¹⁴ the formation of carbon cation was also proposed. However, the reaction between this intermediate and $-\text{NH}_2$ or $-\text{OH}$ was suggested to be the rate-determining step, and therefore, the condensation reactions were concluded to be bimolecular mechanism. Apparently, our

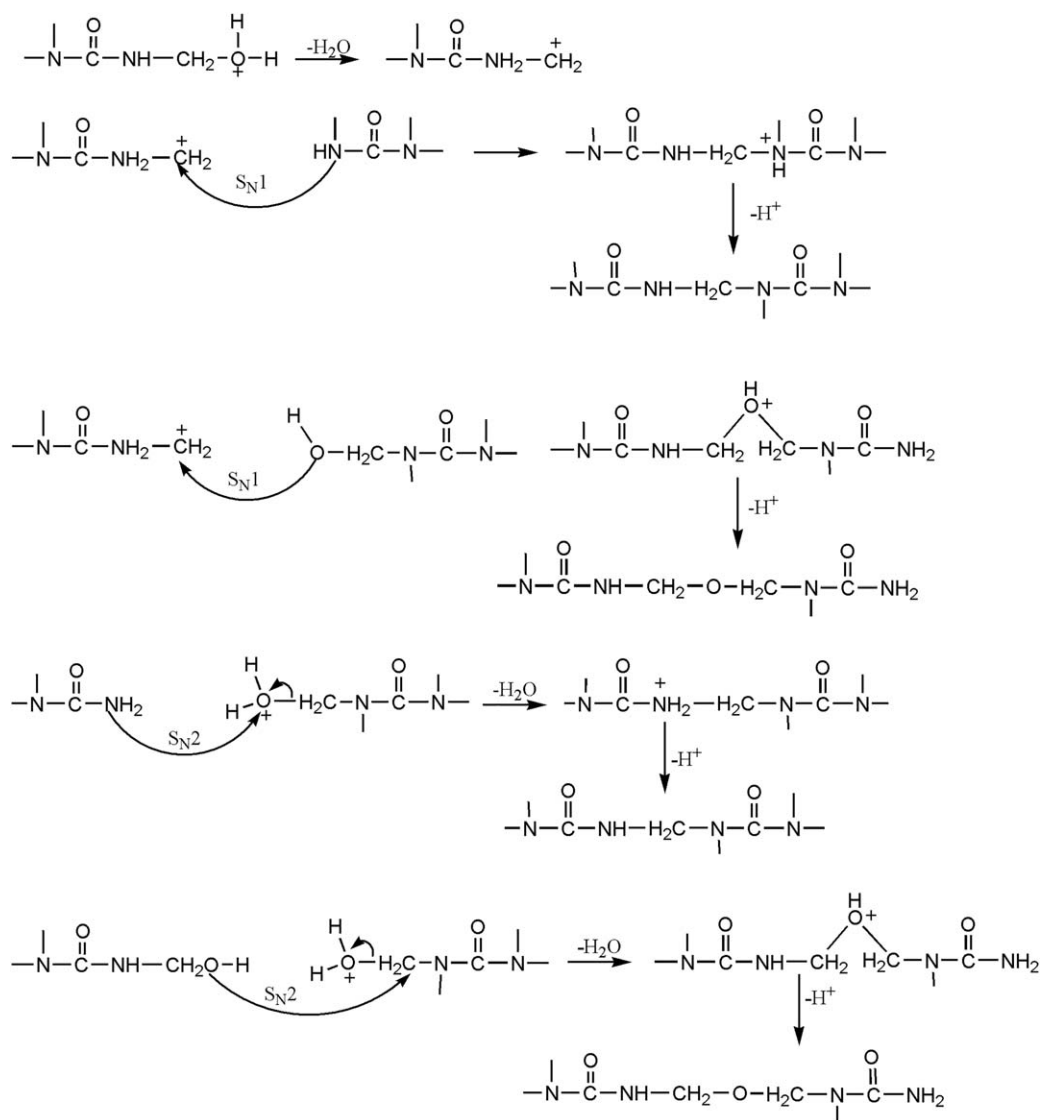


Figure 4. The mechanisms of the acid-catalyzed formation of methylene and methylene ether linkages.

calculations gave a different result. By comparing the energetics shown in Figure 6 with those in Figure 8, it is easy to find that the formation of carbon cation has higher energy barrier than the condensation step. Therefore, the condensations should be monomolecular reactions. How to understand the contradiction between theoretical and experimental results? A plausible explanation is that the energy gap between the two steps is not large enough to distinguish monomolecular mechanism from the bimolecular one. As theoretical calculations predicted that the formation of carbon cation has barrier of 40 kJ/mol with the catalysis of a water molecule, this reaction may undergo efficiently at a temperature slightly above room temperature. In the real solution, with the help of more water molecules, the barrier may be lower and closer to that of the condensation step. Therefore, the close reaction rates of the two steps make the condensation reaction exhibit bimolecular features. Based on the preference of the carbon cation formation, we ruled out the S_N2 mechanism shown in Figure 4.

In the kinetics study on De Jong *et al.*,¹⁴ it was found that the rate constant for the dimethylolurea (UF_2) condensation was 50–20 times smaller than the rate constant of dimethylolurea with U or UF. The authors concluded that the unsubstituted amino group $-NH_2$ is much more reactive toward carbon cation than an amido-methylol group $-NH-CH_2OH$. This means that the nitrogen atom of $-NH_2$ group is more nucleophilic than the nitrogen or oxygen atom of $-NH-CH_2OH$. Another conclusion was that the formation of ether linkage was much slow and may be ignored as UF_2 has two $-NH-CH_2OH$ groups; however, the condensation was measured to be very slow. However, the later studies^{2,23,33} showed that considerable ether linkages can be initially formed and a portion of them then rearrange to methylene linkages with the reaction undergoing. To understand the reactivity of the $-NH-CH_2OH$ group, the reactions between two N,N' -dimethylolureas have also been theoretically investigated. The results are given in Figure 9.

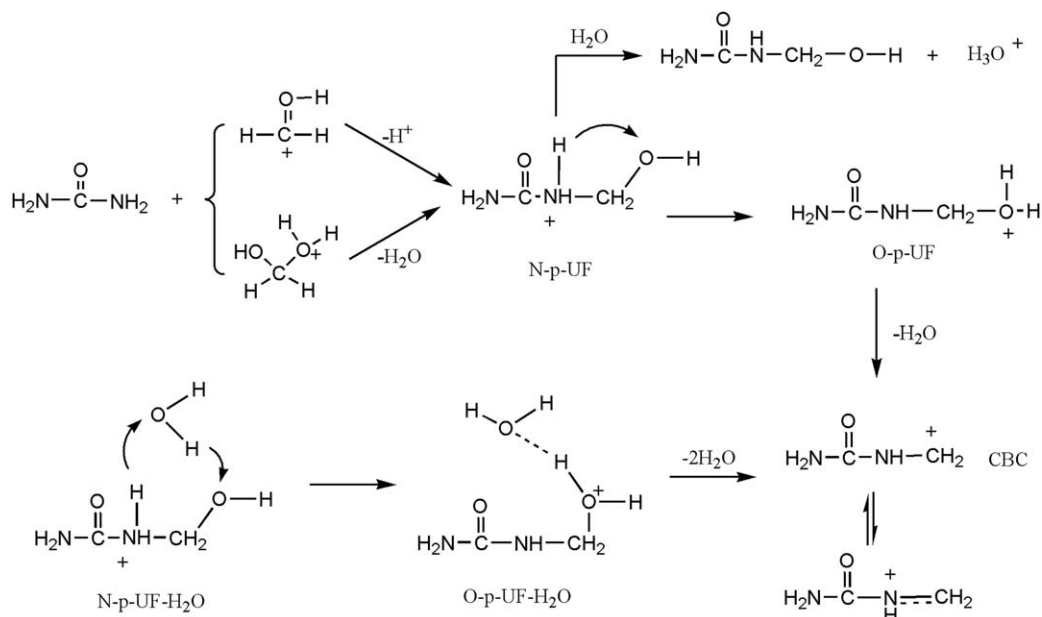


Figure 5. The carbon cation formation mechanism.

As indicated by reactions (9) and (10) in Figure 7, the reactions between dimethylolurea carbon cation (FUF-CBC) and dimethylolurea (UF₂) can form branched methylene linkage or linear

ether linkage. The transition state for reaction (9) was not located despite of numerous searches. This does not mean that this reaction cannot take place. Theoretically, the absence of such

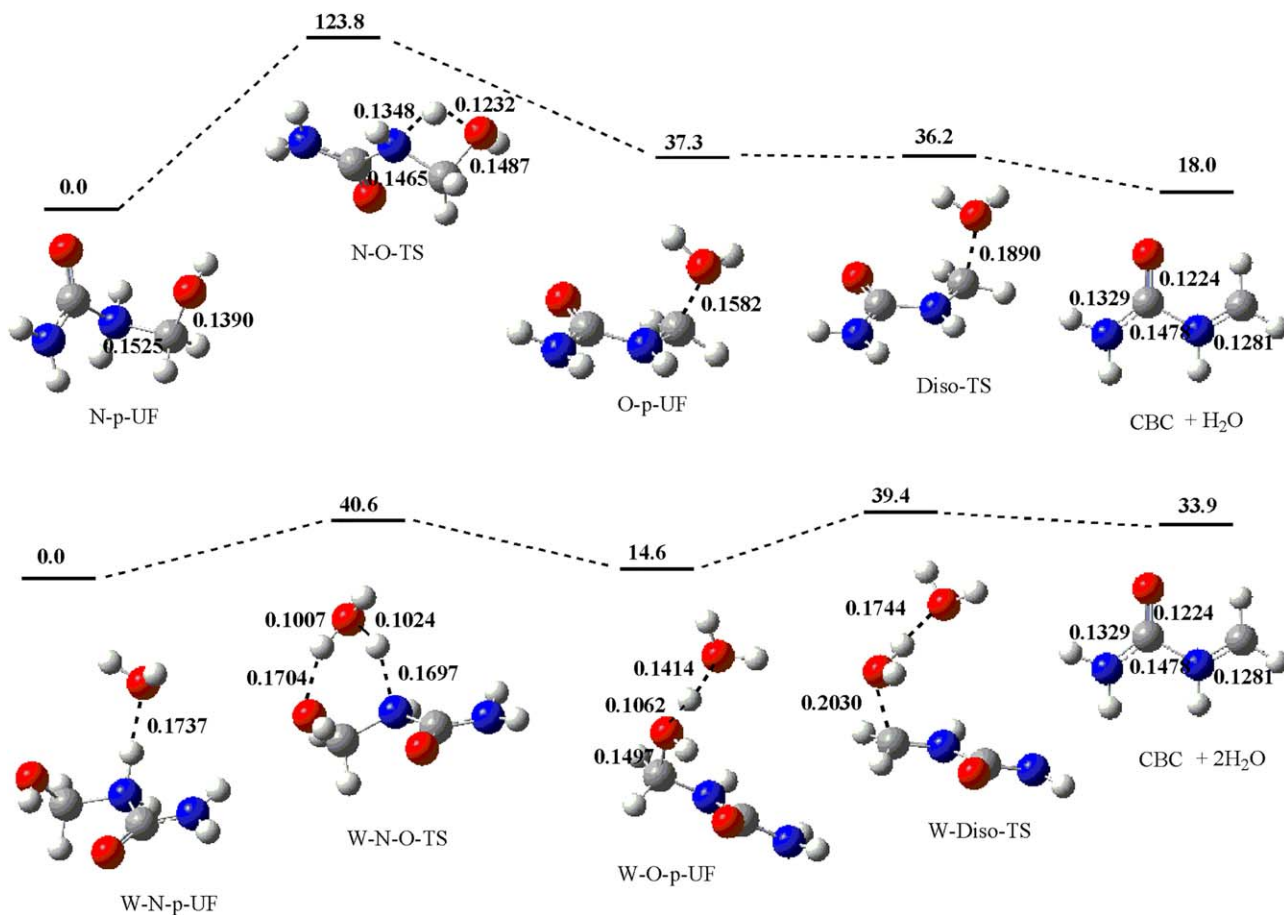


Figure 6. The structures (bond length in nm) and relative energies (kJ/mol) of the stationary points on the PES of the carbon cation formation reaction. [Color figure can be viewed at wileyonlinelibrary.com.]

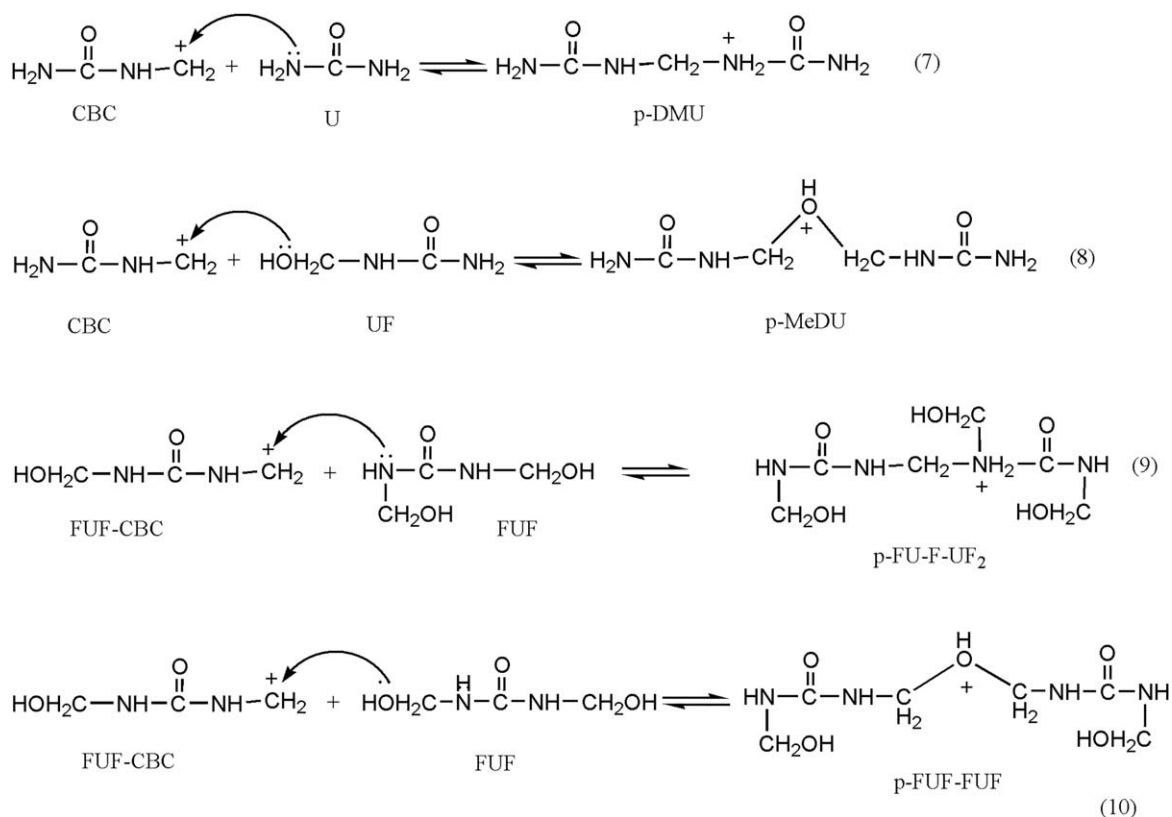


Figure 7. The reactions between carbon cations and methylolureas leading to methylene and methylene ether linkages.

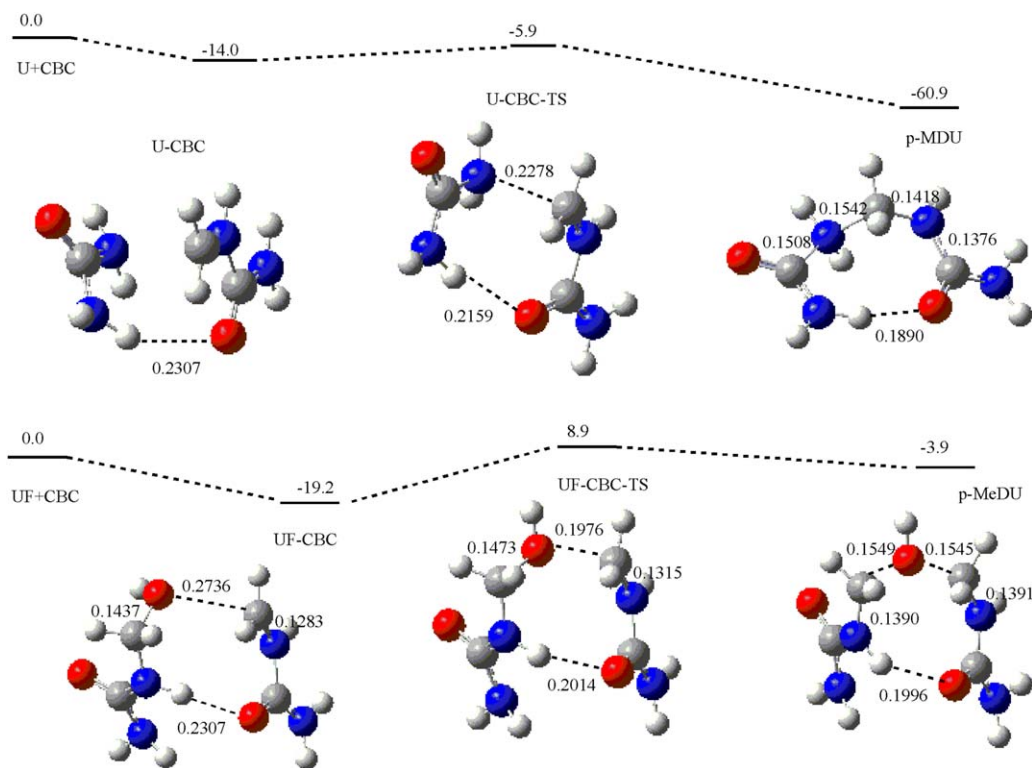


Figure 8. The structures (bond length in nm) and relative energies (kJ/mol) of the stationary points on the PESs of reactions (7) and (8). [Color figure can be viewed at wileyonlinelibrary.com.]

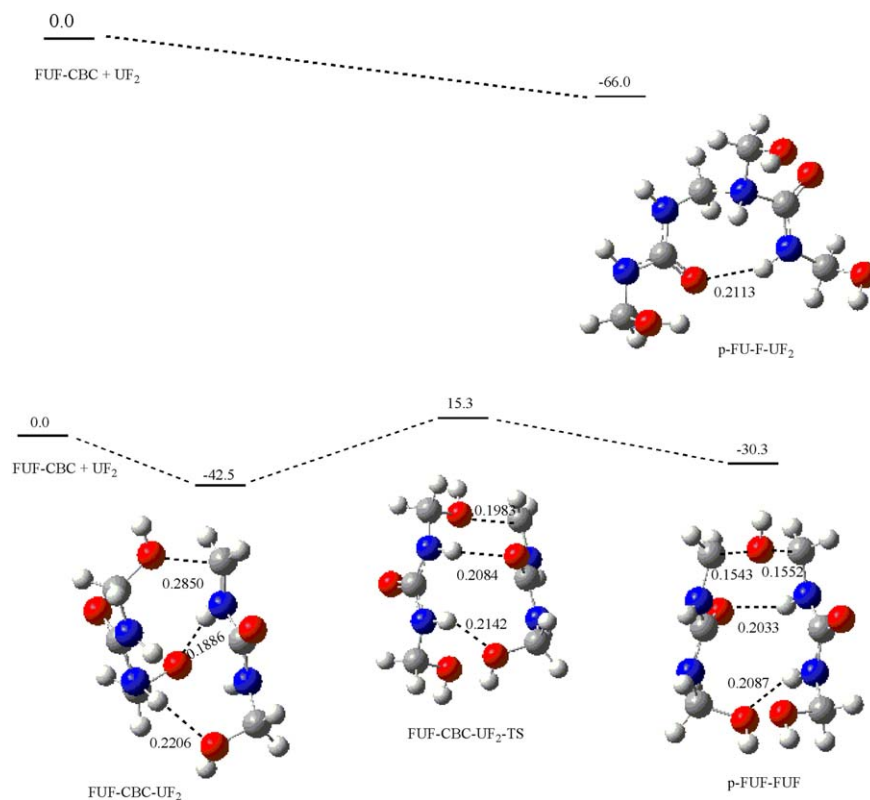
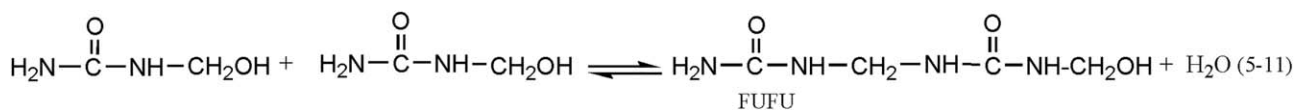
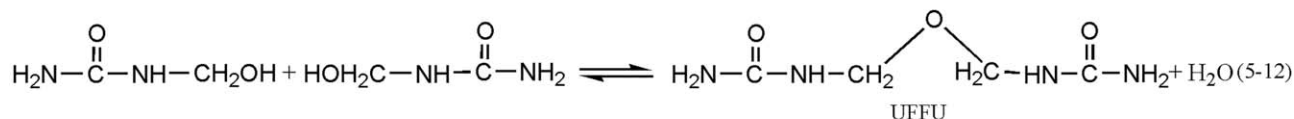


Figure 9. The structures (bond length in nm) and relative energies (kJ/mol) of the stationary points on the PESs of reactions (9) and (10). [Color figure can be viewed at wileyonlinelibrary.com.]



$$\Delta E = -44.3 \text{ kJ/mol} \quad \Delta_r G_m^0 = -30.2 \text{ kJ/mol} \quad \Delta_r H_m^0 = -42.9 \text{ kJ/mol} \quad \Delta_r S_m^0 = -0.04 \text{ kJ/mol}$$



$$\Delta E = -37.0 \text{ kJ/mol} \quad \Delta_r G_m^0 = -21.9 \text{ kJ/mol} \quad \Delta_r H_m^0 = -35.8 \text{ kJ/mol} \quad \Delta_r S_m^0 = -0.05 \text{ kJ/mol}$$

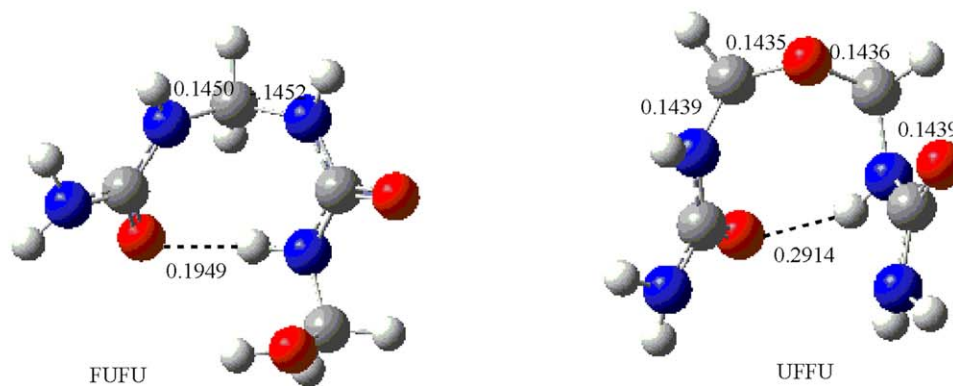


Figure 10. The thermodynamic data and the structures (bond length in nm) of the methylene and methylene ether linked products produced through the condensations of two monomethylureas. [Color figure can be viewed at wileyonlinelibrary.com.]

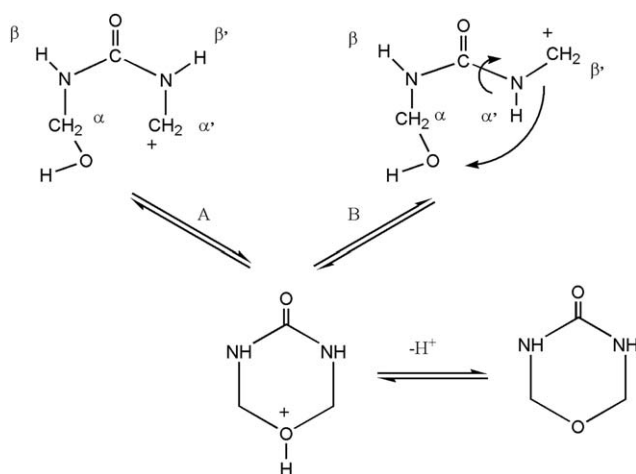


Figure 11. The mechanism of uron formation.

transition state is because the energy barrier on the potential energy surface is too small so that the barrier is ignored. Therefore, this reaction can be almost viewed as a barrierless process. To confirm whether the reaction product exists, geometry optimization was performed. The obtained structure is shown in Figure 9 as p-FU-F-UF₂. The energy of this product is lower than the reactants FUF-CBC + UF₂ by 66.0 kJ/mol, suggesting that it is a stable species like p-MDU in Figure 8 and that the formation of methylene linkage through the reaction between two dimethylolureas is energetically more favorable. The reaction (10) corresponds to the formation of ether linkage through

the reaction between two dimethylolureas. The collision between FUF-CBC with UF₂ initially formed the hydrogen-bonding complex FUF-CBC-UF₂, which is more stable than the reactants by 42.5 kJ/mol. In comparison with UF-CBC, this complex is obviously more stable. The higher stability lies in more hydrogen bonds in the structure. The FUF-CBC-UF₂-TS that represents the barrier of 57.8 kJ/mol is the transition state for the attacking of —CH₂⁺ on —OH. The barrier of this transition state is higher than that of UF-CBC-TS by 27.7 kJ/mol, suggesting that the formation of ether linkage from dimethylolureas is energetically less favorable than the formation from monomethylolurea.

The above calculated results show that either for monomethylolurea or dimethylolurea, the condensations energetically favor the formation of methylene linkage over the ether linkage. However, energy barrier is not the unique factor that influences the reaction rate and product distribution. We prefer that the steric hindrance we proposed for alkaline reactions is also a key factor here that must be considered for the reaction between carbon cation and amido-methylol group —NH—CH₂OH. In such reaction, collisions between the —CH₂⁺ and —NH— group may be suppressed by the steric hindrance caused by —CH₂OH group. In other words, statistically the collision between —CH₂⁺ and —CH₂OH has higher probability than the collision between —CH₂⁺ and —NH—. This means that the formation of branched methylene linkage is energetically favorable; however, the formation of ether linkage is sterically favorable. This speculation can explain the above-mentioned contradiction between the kinetic study of De Jong *et al.*¹⁴ and the later NMR studies.^{2,23,33} First,

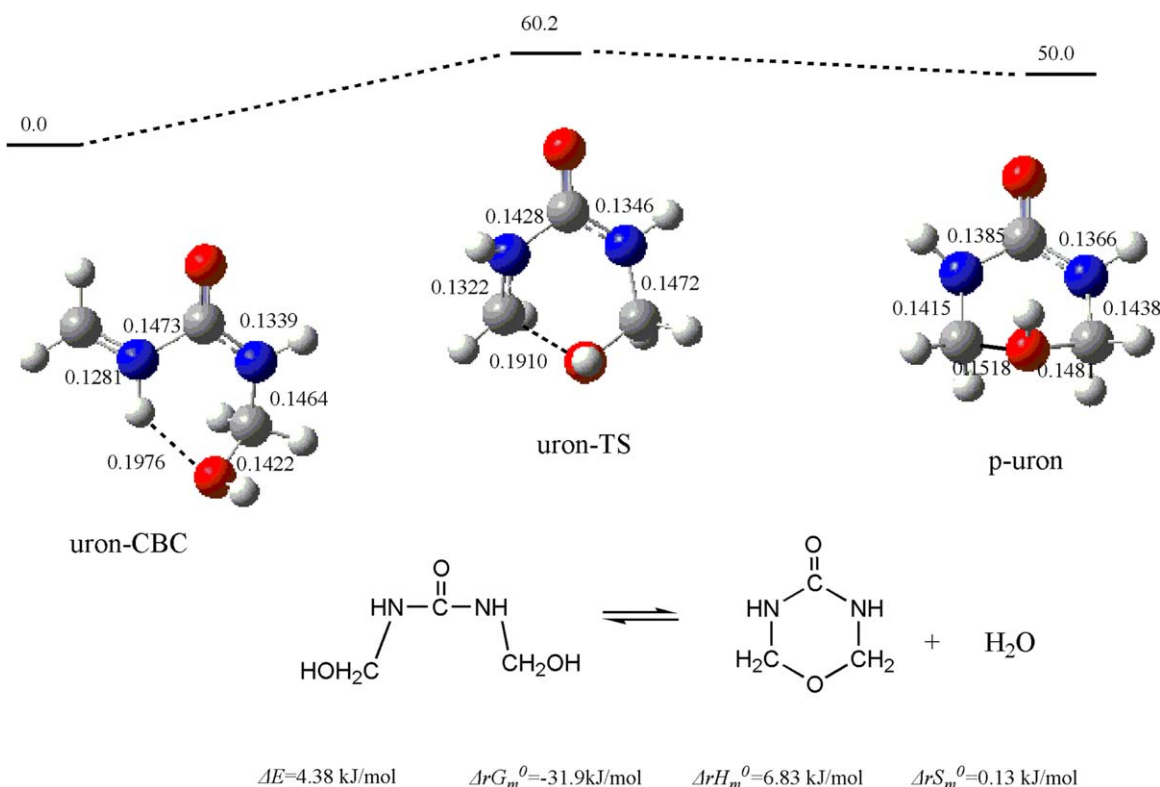


Figure 12. The structures (bond length in nm) and relative energies (kJ/mol) of the stationary points on the PES of uron formation reaction. [Color figure can be viewed at wileyonlinelibrary.com.]

Table I. The Relative Content of the Methylenic and Carbonyl Carbons (%)

Structures	Chemical shifts (δ)	F/U = 2:1				F/U = 1:1	
		UFA-1 (1 h)	UFA-2 (2 h)	UFA-3 (3 h)	UFA-4 (4 h)	UB-1 (0.5 h)	UB-2 (1 h)
$-\text{NH}-\text{CH}_2-\text{NH}-$ (I)	46-48 (45-46) ^a	2.80	5.95	7.24	8.14	26.68	33.56
$-\text{NH}-\text{CH}_2-\text{N}=\text{}$ (II)	53-55 (52-53) ^a	2.35	8.06	21.53	21.36	7.71	12.12
$=\text{N}-\text{CH}_2-\text{N}=\text{}$ (III)	60-61	—	0.67	2.00	2.20	—	—
Total		5.15	14.68	30.77	31.70	34.39	45.68
$-\text{NH}-\text{CH}_2\text{OCH}_2\text{NH}-$ (I)	68-70	13.94	15.85	8.27	7.54	13.40	11.89
$-\text{NH}-\text{CH}_2\text{OCH}_2\text{N}=\text{}$ (II)/ $-\text{CH}_2-$ in unsubstituted uron	75-77	3.52	6.26	5.43	4.58	0.29	—
$=\text{N}-\text{CH}_2\text{OCH}_2\text{N}=\text{}$ (III)/ $-\text{CH}_2-$ in substituted uron	78-80	0.83	1.68	2.26	0.93	—	—
Total		18.29	23.79	15.96	13.05	13.69	11.89
$-\text{NH}-\text{CH}_2\text{OH}$ (I)	64-66	46.15	28.21	16.10	17.20	41.03	31.63
$-\text{N}(-\text{CH}_2)-\text{CH}_2\text{OH}$ (II)	71-72	16.60	17.53	18.03	15.51	2.08	1.62
Total		62.75	45.74	34.13	32.71	43.11	33.32
$\text{HO}-\text{CH}_2-\text{OH}$	83-84	2.38	3.91	6.46	8.47	0.26	0.41
$-\text{OCH}_2-\text{O}-\text{CH}_2-\text{OCH}_2\text{O}-$	86-87	3.92	3.76	5.24	7.46	0.16	—
$-\text{OCH}_2-\text{O}-\text{CH}_2-\text{OCH}_2\text{O}-$	90-91	2.66	2.46	3.36	4.15	0.36	0.26
$\text{H}(\text{CH}_2\text{O})_n\text{OCH}_2\text{OCH}_3$	94-95	0.40	0.51	0.65	0.59	—	0.32
Total		9.36	10.64	15.71	20.67	0.78	0.99
$-\text{NH}-\text{CH}_2-\text{O}-\text{CH}_3$	72-73	4.44	5.16	3.43	1.86	8.03	8.11
$\text{NH}_2-\text{CO}-\text{NH}_2$	163-164 (161-162) ^a	0.66	0.16	—	—	12.30	9.27
$\text{NH}_2-\text{CO}-\text{NH}-$	161-162 (160-161) ^a	17.86	12.67	5.33	7.23	52.31	54.77
$-\text{NH}-\text{CO}-\text{N}-/-\text{NH}-\text{CO}-\text{N}=\text{}$	159-161 (158-160) ^a	81.20	87.10	94.42	92.77	35.39	35.96
Uron	154-158	0.28	0.08	0.25	—	—	—

^a 1-2 ppm movement to high field occurred for UFB-1 and UFB-2 because more DMSO- d_6 was used.

in the kinetic study of De Jong *et al.*, the highest reaction temperature was 50 °C. This relatively low temperature cannot provide enough energy to overcome the barrier for condensations of UF₂ to form ether linkages. Meanwhile, condensations to form methylene linkages were also slow due to the steric hindrance. Differently, in the synthesis of UF resins, the condensations are allowed to occur at around 90 °C that guarantees the collision energy to overcome the barrier for ether linkage formation. Therefore, at the initial stage of the condensations, the ether linkages were always observed to be preferred, especially when the F/U molar ratio was 2/1 or above. In fact, it has been widely accepted that the condensations under acidic condition mainly form ether linkages at the initial stage and a part of them can rearrange to methylene linkages as the reactions undergo. However, on the basis of our calculations and speculation on steric hindrance, we believe that the dominant formation of ether linkages at the initial stage of condensation is not definite. Theoretically, when the F/U molar ratio is controlled to

be 1/1 or lower, monomethylolurea would be the main product and the reaction between free amino group $-\text{NH}_2$ and $-\text{CH}_2^+$ becomes dominant as such reaction is not influenced by steric hindrance. To elucidate the competitive relationship between methylene and methylene ether linkages and the influence of the molar ratio, experiments were designed and the results were discussed in the following section.

The phenomenon of ether linkage rearranging to methylene linkage implies that the latter is also thermodynamically more stable. To confirm this, theoretical calculations were also performed on the thermodynamic properties of the two types of condensations. The results are shown in Figure 10. The condensation of two monomethylolureas can produce FUFU or UFFU and they are isomers. The formation of FUFU is exothermic by 44.3 kJ/mol (ΔE), which is more exothermic than the formation of UFFU by 7.3 kJ/mol, suggesting that methylene linkage product is more stable than the ether linkage product. The ΔG_m^0

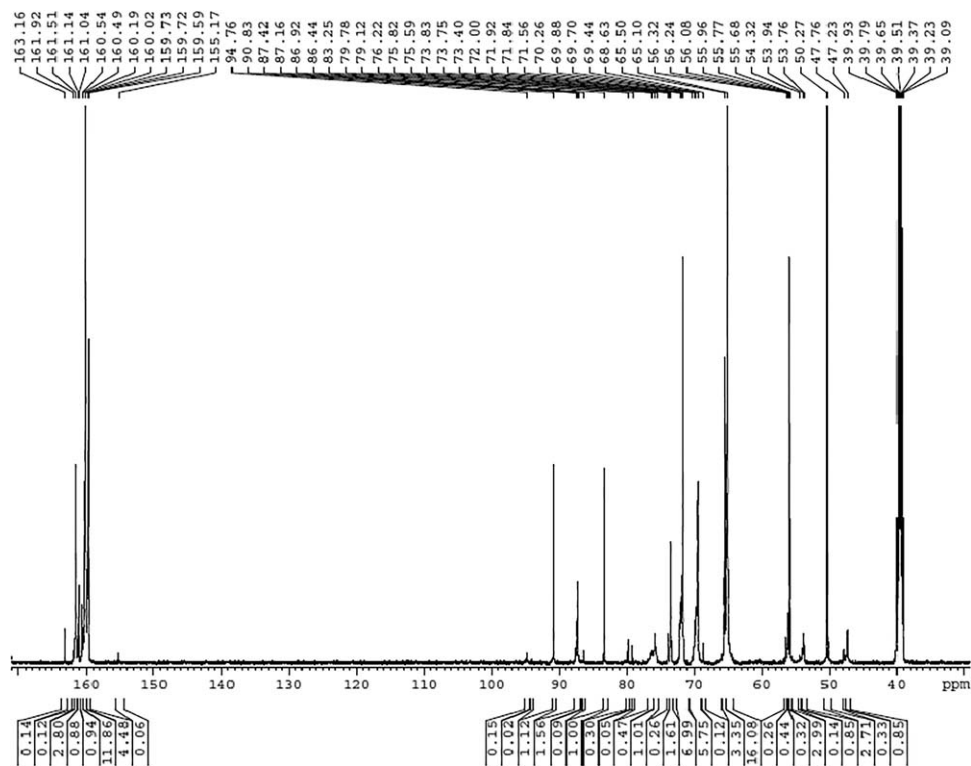


Figure 13. The ^{13}C -NMR spectrum of sample UFA-1.

(298.155 K) for FUFU is also more negative than UFFU by 7.1 kJ/mol, indicating that the former is indeed thermodynamically more favorable.

The uron was previously proposed to be produced through intramolecular water elimination. According to the intermolecular condensation mechanism identified in this work, the formation of

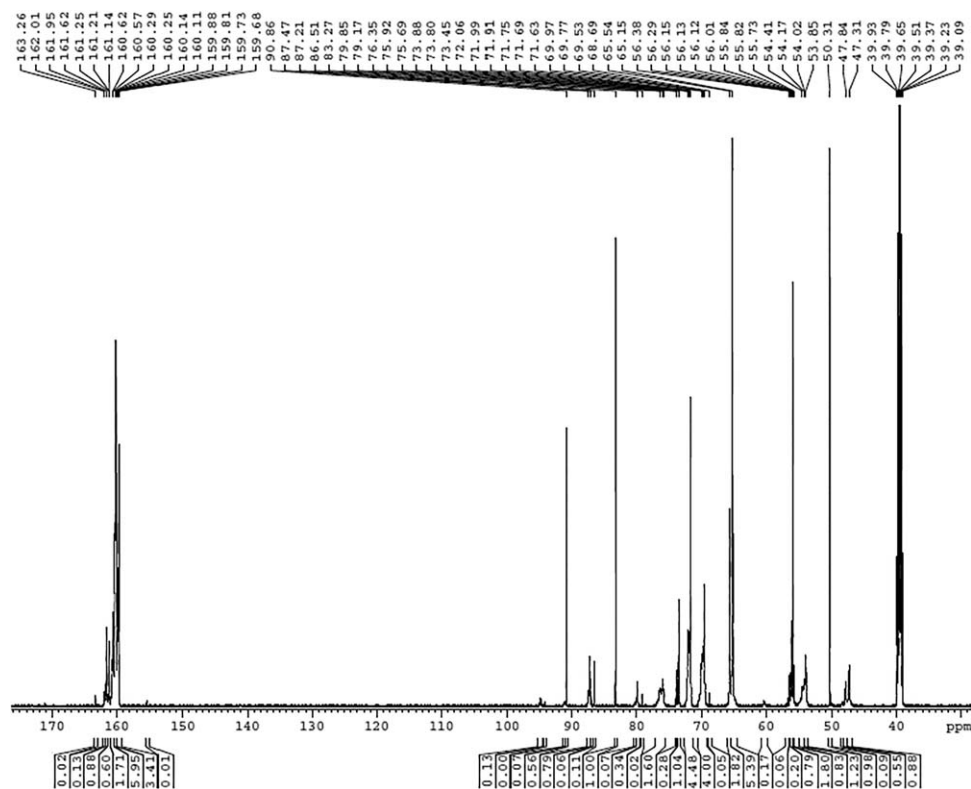


Figure 14. The ^{13}C -NMR spectrum of sample UFA-2.

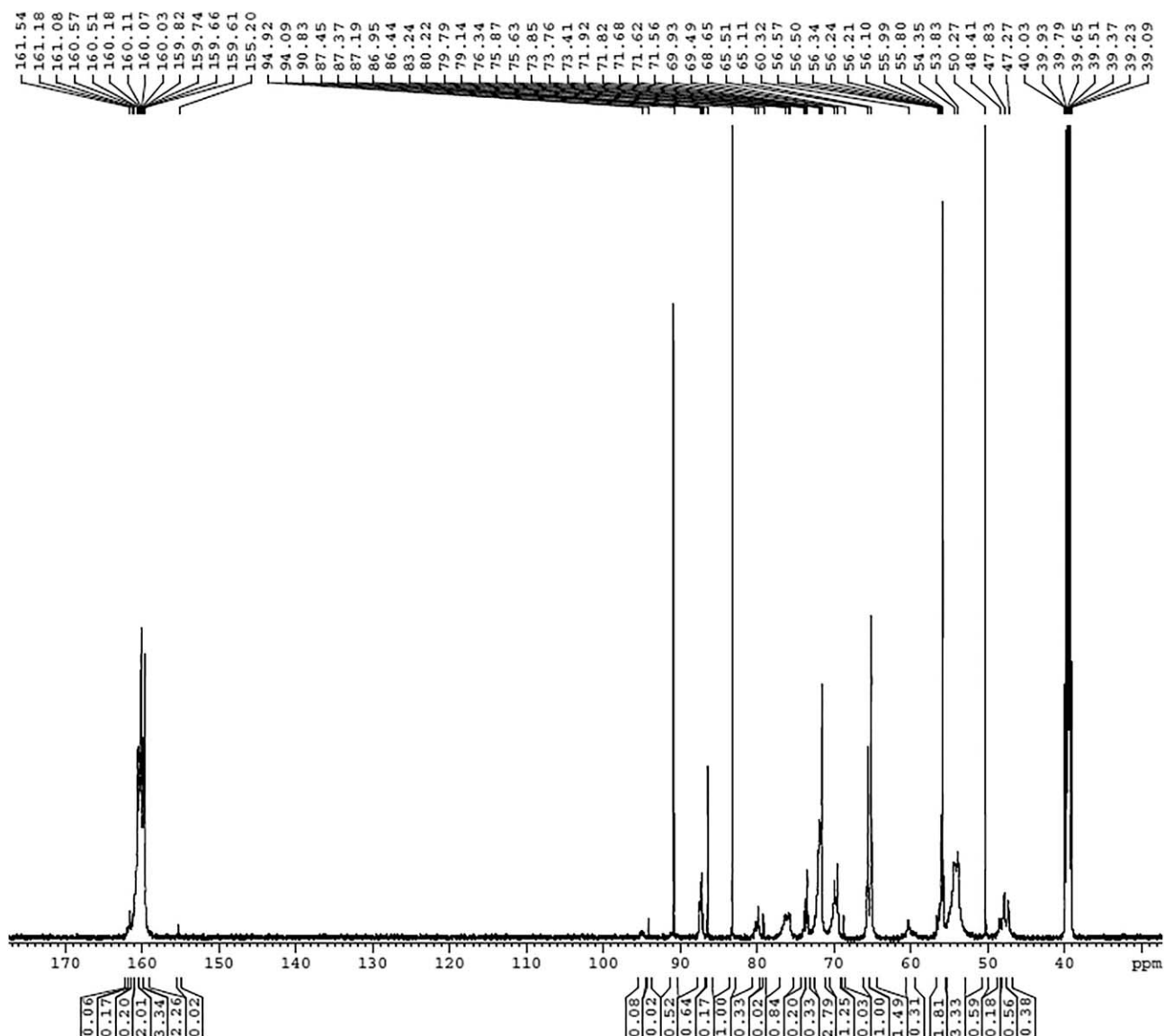


Figure 15. The ^{13}C -NMR spectrum of sample UFA-3.

uron also involves the carbon cation intermediate. The mechanism is shown in Figure 11. Ideally, the uron should be produced from α,α' - N,N' -dimethylolurea which has *cis*-conformation. The corresponding carbon cation should also have a *cis*-structure. However, theoretical calculations excluded the existence of such intermediate. Instead, the *trans*- α,β' carbon cation was located. Its structure is shown in Figure 12 as uron-CBC. By rotating the C—N bond (0.1473 nm), the carbon can attack the —OH group to form cyclic structure. This step has barrier of 60.2 kJ/mol that is represented by the transition state uron-TS. Obviously, this reaction has much higher barrier than reactions (7) and (8), and therefore, the formation of uron should be much slower than intermolecular condensations. This is in agreement with the general experimental observations.^{21–24,31–33} However, considerable uron structures were observed under strong acidic condition.^{31–33} This implies that the formation of uron is kinetically unfavorable but thermodynamically allowed as our calculations predicted the ΔG_m^0 for uron to be -31.9 kJ/mol.

^{13}C -NMR Results and Analysis

Table I shows the ^{13}C -NMR quantitative results for the samples. UFA and UFB series correspond to F/U = 2/1 and 1/1, respectively. Chemical shifts were assigned by referencing the reported literatures.^{20–24} The relative contents of different methylenic carbons were calculated for the structures list in this table using the integral values in Figures 13–18.

For UFA-1 which was taken at reaction time of 1 h, the total content of methylene ether carbons accounts for 18.29%, among which the type I linear ether linkage (around 69 ppm) carbon dominantly accounts for 13.94%. In contrast, the total content of methylene linkage carbons shows a lower percentage of 5.15%. This clearly indicates that the formation of ether linkages is a competitive process and is faster than the formation of methylene linkages at the initial stage of condensations. In UFA-2 (2 h), the content of ether linkage carbons increased to 23.79%, which is the highest percentage during the whole condensation stage. Meanwhile, the content of methylene linkages increased to 14.68%. This

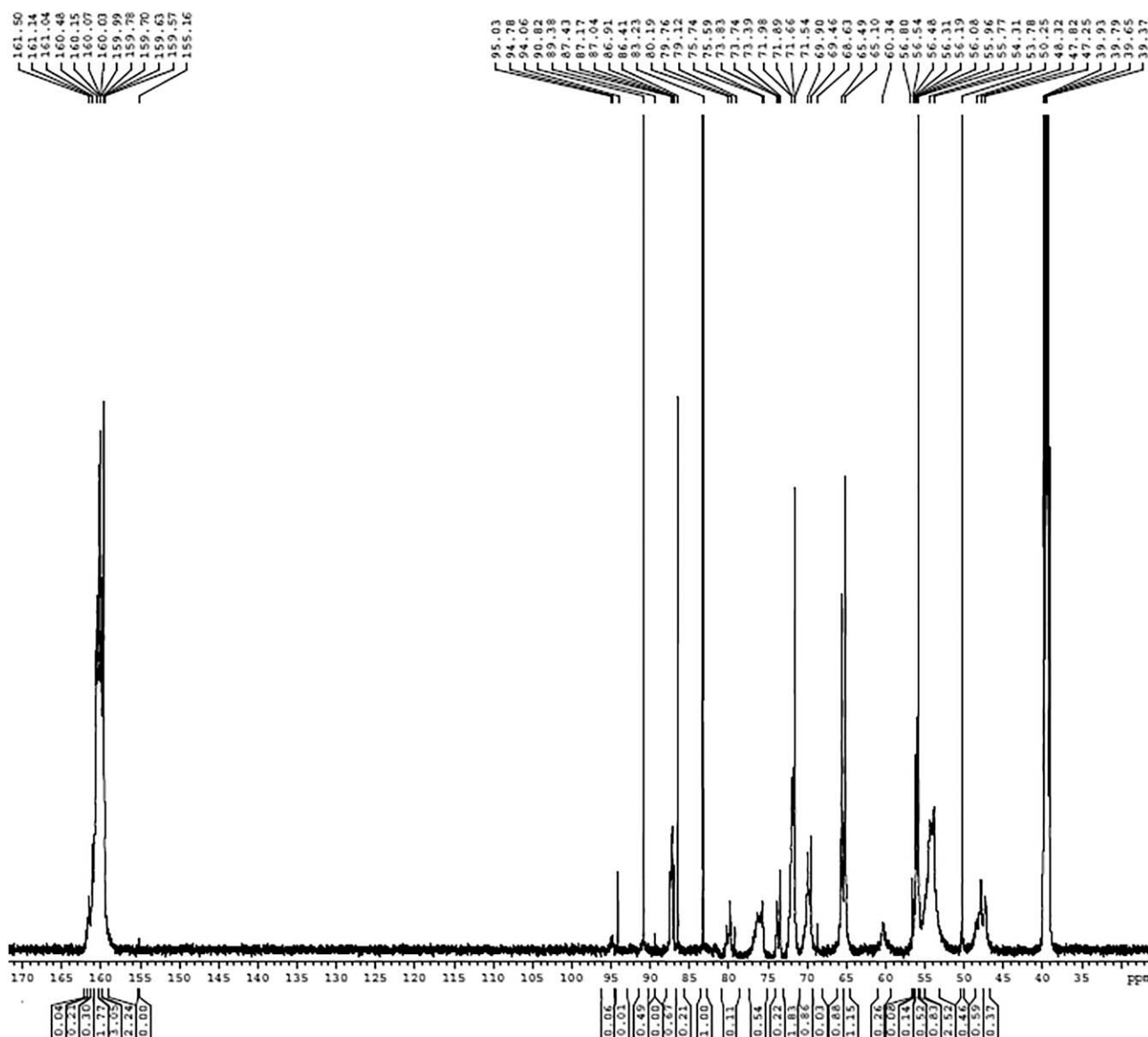


Figure 16. The ^{13}C -NMR spectrum of sample UFA-4.

implies that the formation of methylene linkages is a simultaneous process and does not rely on the initial formation of ether linkages. With the reaction undergoing, the content of ether linkage carbons decreased to 15.96% in UFA-3. Particularly, the linear ether linkage carbon significantly decreased by 7.58%. With the significant decrease of ether linkages, the total content of methylene linkages rapidly increased to 30.77%. The current theory states that these structure changes correspond to the rearrangement of a part of ether linkages to methylene linkages. An interesting issue is that the rearrangement is always accompanied by increment of the formaldehyde, as it can be seen in Table I that the total content of formaldehyde increased from 10.64 to 15.71%. Based on these changes, the rearrangement mechanism was simply proposed as reaction (a) in Figure 19. This mechanism has been widely cited in numerous literatures. Recently, Sun *et al.*³³ proposed more detailed mechanism for the acid-catalyzed rearrangement as shown in the same figure as reaction (b). Such mechanism seems reasonable and can

also explain the emission of formaldehyde during rearrangement. However, our calculations found that step B, which corresponds to the breakage of C—O bond, has an energy barrier of 163.9 kJ/mol. This notable barrier indicates such reaction is inefficient even at high temperature. Suppose this reaction can occur, linear ether linkage should convert to linear methylene linkage. However, obviously, this is not consistent with the ^{13}C -NMR observations. It can be seen in Table I that the type I methylene linkage (around 47 ppm) only increased by 1.29% from UFA-2 to UFA-3; however, the type I ether linkage decreased by 7.58%. Furthermore, from UFA-2 to UFA-3, the increment of methylene linkage carbons was mainly contributed by the type II branched linkages (around 54 ppm). This type of linkage obviously cannot be formed from the mechanism suggested by Sun *et al.* Therefore, there must be another mechanism. Based on the ^{13}C -NMR results and theoretical calculations, we proposed other possible rearrangement pathways and they are shown in Figure 20.

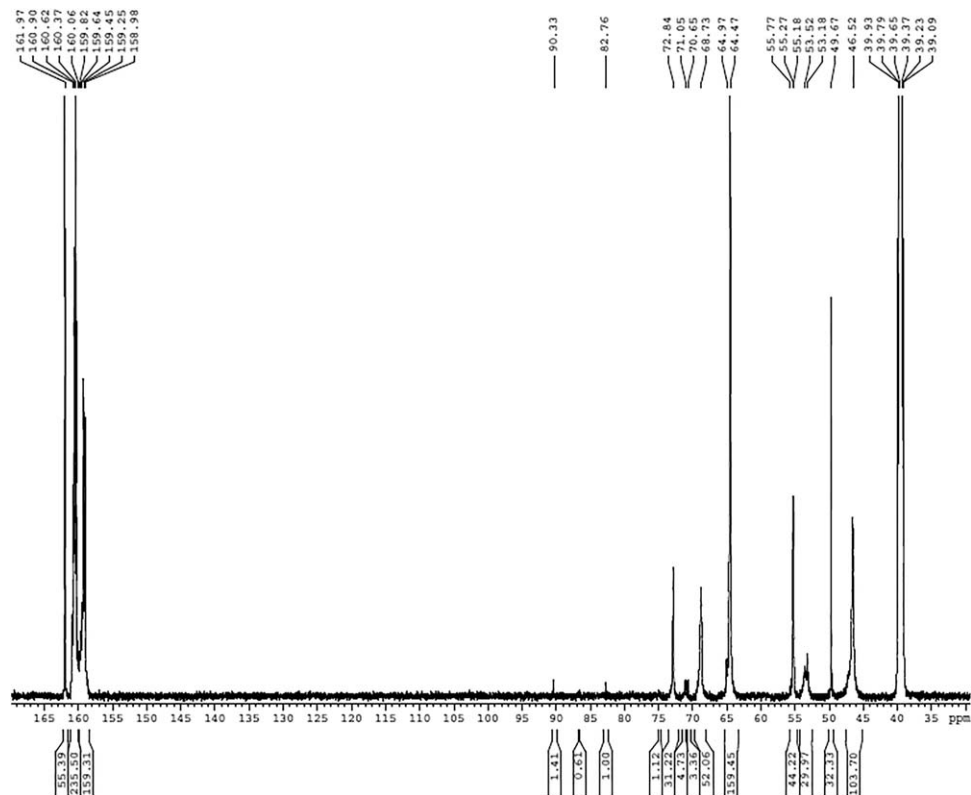


Figure 17. The ^{13}C -NMR spectrum of sample UFB-1.

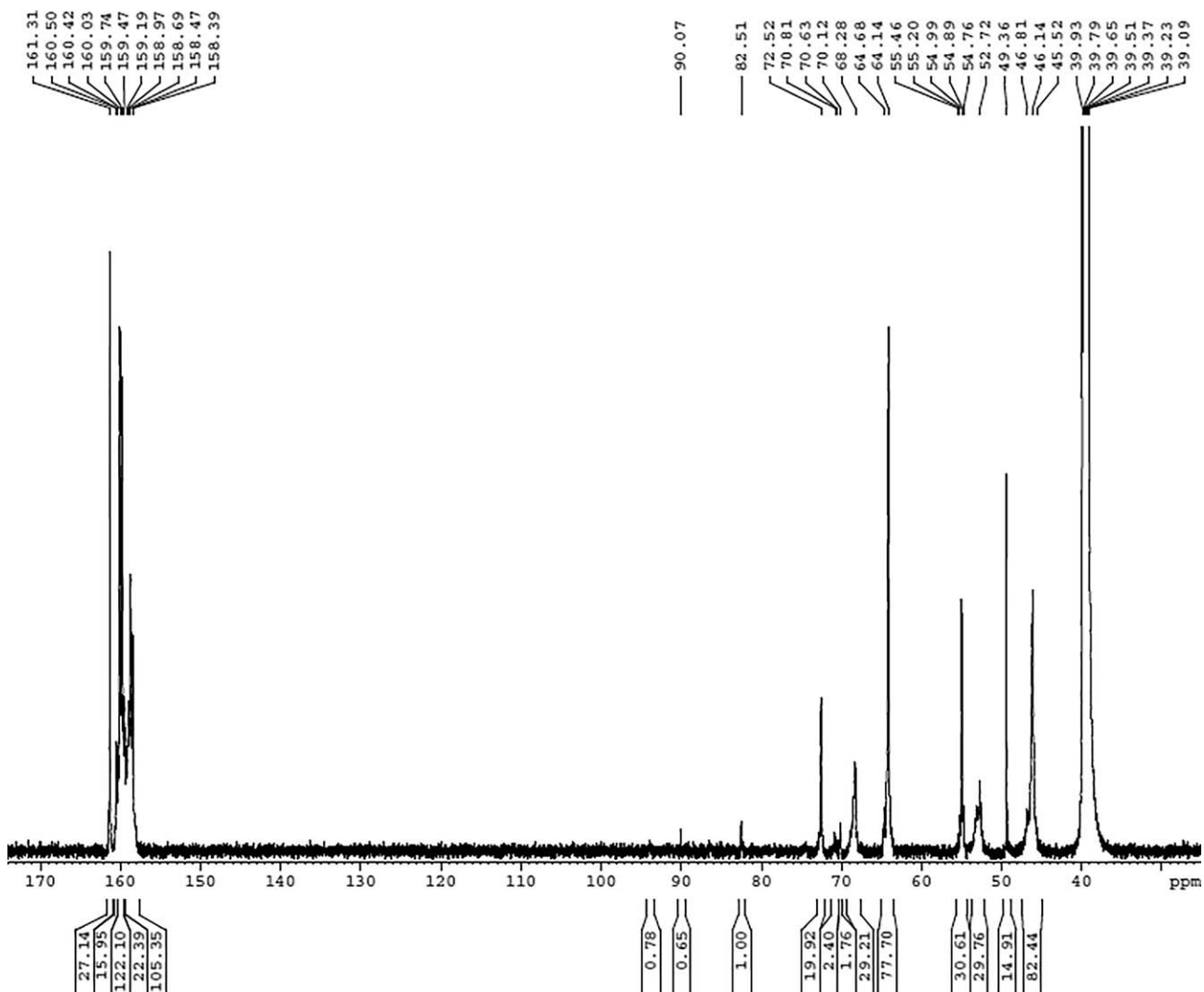


Figure 18. The ^{13}C -NMR spectrum of sample UFB-2.

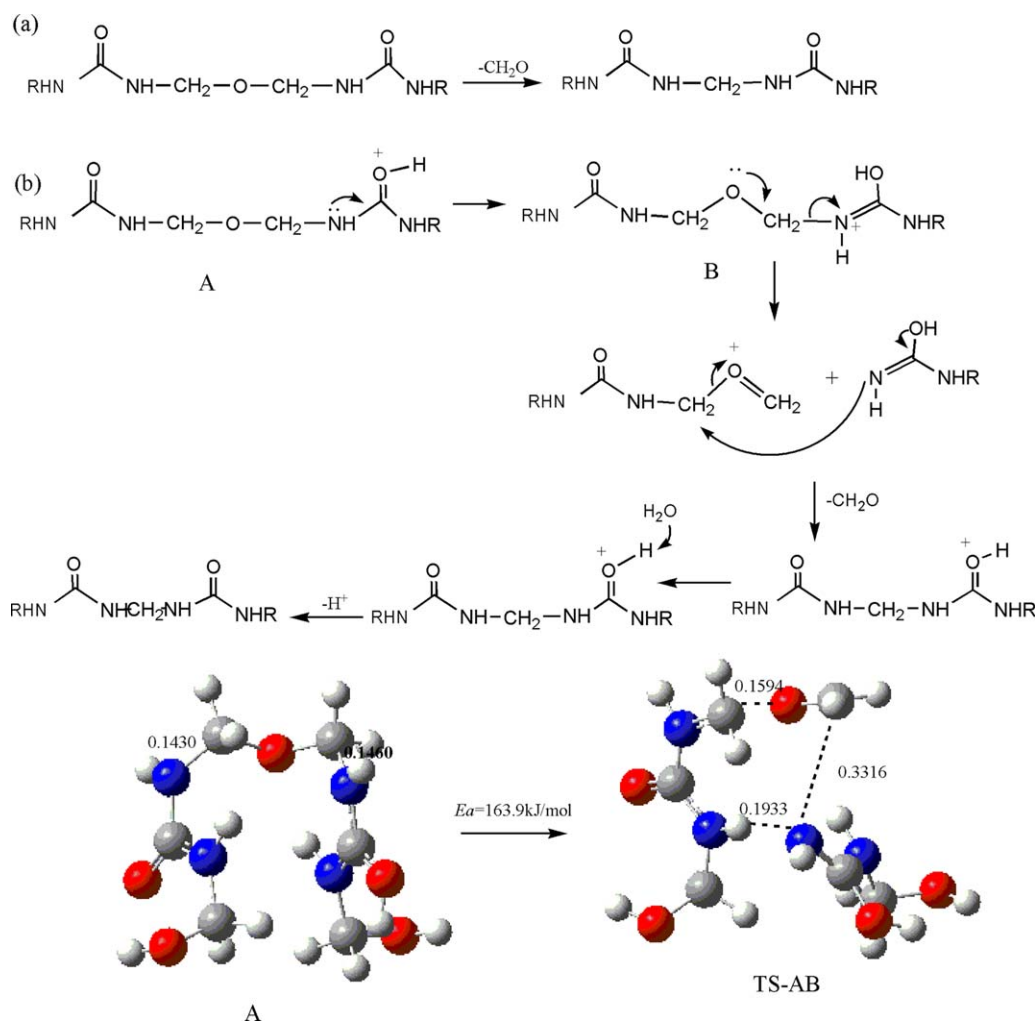


Figure 19. The previously proposed mechanism for the rearrangement of methylene ether linkage to methylene linkage (Ref. 33). [Color figure can be viewed at wileyonlinelibrary.com.]

The driving force of the rearrangement is that the methylene linkage is thermodynamically more stable than ether linkage. At the initial stage of condensation, the steric hindrance suppresses the reaction between two $-\text{NH}-\text{CH}_2\text{OH}$ groups to form methylene linkage, and therefore, the formation of ether linkage is faster. With the reactions undergoing, the equilibrium would shift to the formation of methylene linkages. From this sense, polymers linked with ether linkages are only intermediate products with respect to the more stable polymers linked with methylene linkages. Figure 20 shows a model that demonstrates different rearranging routes of a dimethylolurea dimer. In the first route, the linear dimer decomposes to two dimethylolureas, which subsequently recollide to form the branched methylene linkage isomer. As discussed above, this reaction may be slower due to the steric hindrance; however, this effect does not change the thermodynamic nature of the equilibrium. Such mechanism can rationalize the phenomenon that the decrease of type I ether linkage corresponds to the rapid increment of the type II methylene linkage at the later condensation stage. It seems that this pattern of rearrangement does not emit formaldehyde and cannot explain the increased content of the

formaldehyde. However, according to our understanding, directly relating the emission of formaldehyde to the rearrangement may be a mistake. With respect to equilibrium, the condensations leading to methylene linkages consume primary ($-\text{NH}_2$) or secondary ($-\text{NH}-$) group and therefore changes the methylation–demethylation equilibrium. Thus, the decrease of reactive protons on amino group directly leads to more free formaldehyde. Therefore, the above mechanism still stands. Another rearranging route shown in Figure 20 is more circuitous and may not be the dominant one.

As the steric hindrance is speculated to be an important factor that influences the competitive relationship of the methylene and methylene ether linkages at the initial stage of condensation, it is necessary to find out experimental evidence. As shown in Table I, when the F/U molar ratio was lowered to be 1/1, different situations were found. Within a short reaction time of 0.5 h, 34.39% formaldehyde has been converted into different types of methylene linkage carbons. In contrast, the methylene ether carbons accounted only for 13.69%. This result clearly shows that the formation of methylene linkages is faster even at

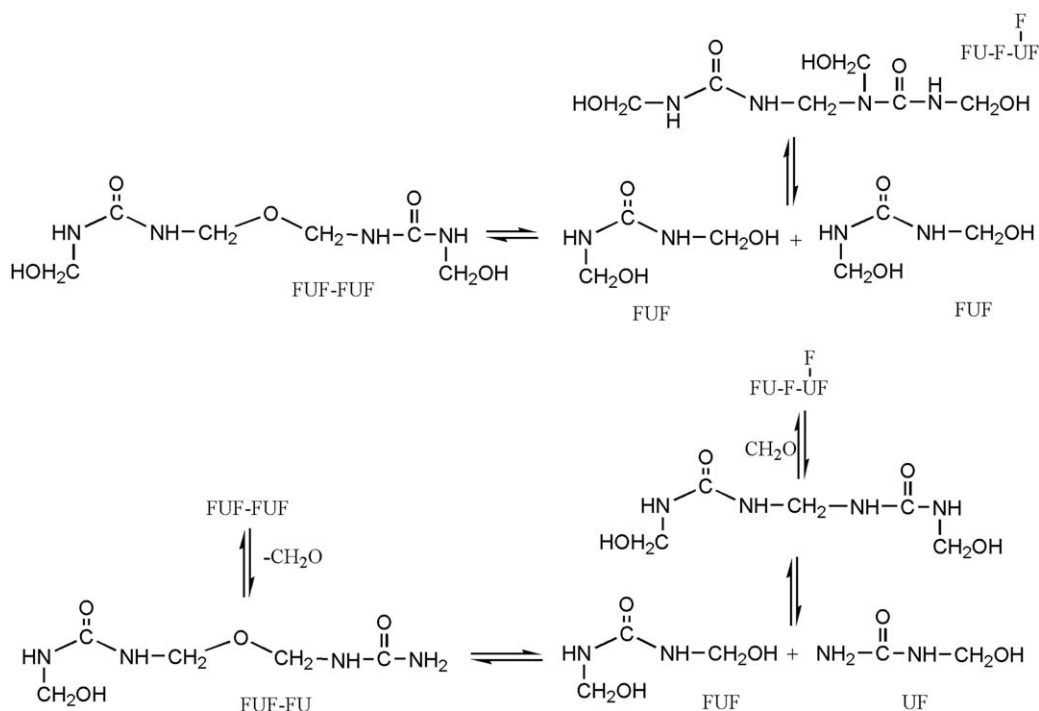


Figure 20. The proposed routes for the conversion of methylene ether linkage into methylene linkage in this work.

the initial stage of condensation, and this situation is totally different from that of $F/U = 2/1$. Because of the low molar ratio, condensations occurred mainly between free amino group ($-\text{NH}_2$) and methylol group ($-\text{CH}_2\text{OH}$) and resulted in mainly the type I linear methylene linkage which dominantly accounts for 26.68%. Obviously, this experimental result confirmed our speculation on steric hindrance effect.

Another interesting issue in condensation stage is the formation of uron and its derivatives. The data list in Table I shows that the contents of uron species are lower than 1% during the whole condensation for the case of 2/1 molar ratio. This agrees with our calculations that the uron formation is kinetically much less favorable than intermolecular condensations. For 1/1 molar ratio, the uron species are absent due to lower contents of di- and tri-methylolureas. However, as our calculations indicated, the formation of uron is thermodynamically allowed. Once a strong acidic condition or enough reaction time is satisfied, higher content of uron can be observed.

CONCLUSIONS

The acid-catalyzed urea–formaldehyde reactions were reexamined in detail by using quantum chemistry method and ^{13}C -NMR determinations. The main conclusions were drawn as follows:

1. Both formaldehyde and methanediol may participate in methylation reactions in protonated form; however, the calculated potential energy barriers suggest that methanediol plays a dominant role.
2. The identified reaction mechanisms and calculated energy barriers indicate that the condensation reactions occur in $\text{S}_{\text{N}}1$ mechanism. The formation of carbon cation intermediate can be catalyzed by solvent water molecule.

3. The condensation reaction between two N,N' -dimethylolureas leading to methylene linkage has lower energy barrier than the reaction leading to methylene ether linkage; however, the former reaction may be suppressed by steric hindrance effect. In contrast, reaction of free amino group with hydroxymethyl group is not influenced by such effect. The ^{13}C -NMR determinations showed that the formation of methylene ether linkages at the initial stage was faster than that of methylene linkages when F/U molar ratio was 2/1. Differently, the formation of methylene linkages became dominant at the initial stage when the F/U molar ratio was lowered to 1/1. The experimental results confirmed our inference that the competitive relationship between the two types of linkages is kinetically controlled by steric hindrance. However, due to the fact that the methylene linkages are thermodynamically more stable than methylene ether linkages, the former always become dominant at the later stage of condensations either with high or low molar ratio.
4. It was found that the previously proposed mechanism for conversion of methylene ether linkage to methylene linkage cannot explain the structural changes during condensations and other mechanisms were proposed.
5. The calculated higher energy barrier suggests that the uron structure formation should be much slower than the intermolecular condensations, which rationalized the experimental result that urons were found in relatively higher content under strong acidic condition.

ACKNOWLEDGMENTS

This work is supported by the programs of National Science Foundation of China (31360159 and 51273163) and the program of Doctoral Scientific Research of Southwest Forestry University.

REFERENCES

1. Dunky, M. *Macromol. Symp.* **2004**, *217*, 417.
2. Dunky, M. *Int. J. Adhes. Adhes.* **1998**, *18*, 95.
3. Despres, A.; Pizzi, A.; Pasch, H.; Kandelbauer, A. *J. Appl. Polym. Sci.* **2007**, *106*, 1106.
4. Sun, Q. N.; Hse, C. Y.; Shupe, T. F. *J. Appl. Polym. Sci.* **2011**, *119*, 3538.
5. Kamoun, C.; Pizzi, A.; Zanetti, M. *J. Appl. Polym. Sci.* **2003**, *90*, 203.
6. Park, B. D.; Lee, S. M.; Roh, J. K. *Eur. J. Wood Wood Prod.* **2009**, *69*, 121.
7. No, B. Y.; Kim, M. G. *J. Appl. Polym. Sci.* **2007**, *106*, 4148.
8. Hse, C. Y. *Forest Prod. J.* **2009**, *59*, 19.
9. No, B. Y.; Kim, M. G. *J. Appl. Polym. Sci.* **2005**, *97*, 377.
10. De Jong, J. I.; De Jong, J. *Recl. Trav. Chim. Pays-Bas* **1952**, *71*, 643.
11. De Jong, J. I.; De Jong, J. *Recl. Trav. Chim. Pays-Bas* **1952**, *71*, 661.
12. De Jong, J. I.; De Jong, J. *Recl. Trav. Chim. Pays-Bas* **1952**, *71*, 890.
13. De Jong, J. I.; De Jong, J. *Recl. Trav. Chim. Pays-Bas* **1952**, *72*, 207.
14. De Jong, J. I.; De Jong, J. *Recl. Trav. Chim. Pays-Bas* **1953**, *72*, 139.
15. Steinhof, O.; Kibrik, E. J.; Scherr, G.; Hasse, H. *Magn. Reson. Chem.* **2014**, *52*, 138.
16. Kibrik, E. J.; Steinhof, O.; Scherr, G.; Thiel, W. R.; Hasse, H. *J. Polym. Res.* **2013**, *20*, 79.
17. Kibrik, E. J.; Steinhof, O.; Scherr, G.; Thiel, W. R.; Hasse, H. *Ind. Eng. Chem. Res.* **2014**, *53*, 12602.
18. Kibrik, E. J.; Steinhof, O.; Scherr, G.; Thiel, W. R.; Hasse, H. *J. Appl. Polym. Sci.* **2012**, *128*, 3957.
19. Christjanson, P.; Siimer, K.; Pehk, T.; Lasn, I. *Holz. Roh. Werkst.* **2002**, *60*, 379.
20. Kim, M. G. *J. Appl. Polym. Sci.* **2001**, *80*, 2800.
21. Kim, M. G. *J. Polym. Sci. Part A: Polym. Chem.* **1999**, *37*, 995.
22. Kim, M. G. *J. Appl. Polym. Sci.* **2000**, *75*, 1243.
23. Siimer, K.; Pehk, T.; Christjanson, P. *Macromol. Symp.* **1999**, *148*, 149.
24. Christjanson, P.; Pehk, T.; Siimer, K. *J. Appl. Polym. Sci.* **2006**, *100*, 1673.
25. Chuang, I.; Maciel, G. E. *J. Appl. Polym. Sci.* **1994**, *52*, 1637.
26. Tomita, B.; Hatono, S. *J. Polym. Sci. Polym. Chem. Ed.* **1978**, *16*, 509.
27. Chiavarini, M.; Fanti, N. D.; Bigatto, R. *Angew. Makromol. Chem.* **1975**, *46*, 151.
28. Chiavarini, M.; Fanti, N. D.; Bigatto, R. *Angew. Makromol. Chem.* **1978**, *70*, 49.
29. Jada, S. *J. Appl. Polym. Sci.* **1998**, *35*, 1573.
30. Li, T.; Guo, X.; Liang, J.; Wang, H.; Xie, X.; Du, G. *Wood Sci. Technol.* **2015**, *49*, 475.
31. Gu, J. Y.; Mitsuo, H.; Mitsuhito, M. H.; Hse, C. Y. *Jpn. Wood Res. Soc.* **1995**, *42*, 483.
32. Soulard, C.; Kamoun, C.; Pizzi, A. *J. Appl. Polym. Sci.* **1999**, *72*, 277.
33. Sun, Q. N.; Hse, C. Y.; Shupe, T. F. *J. Appl. Polym. Sci.* **2014**, *131*, DOI: 10.1002/app.40644.
34. Head-Gordon, M.; Pople, J. A.; Frisch, M. J. *Chem. Phys. Lett.* **1988**, *153*, 503.
35. Miertus, S.; Tomasi, J. *J. Chem. Phys.* **1982**, *65*, 239.
36. Miertus, S.; Scrocco, E.; Tomasi, J. *J. Chem. Phys.* **1981**, *55*, 117.
37. Cossi, M.; Barone, V.; Mennucci, B. *Chem. Phys. Lett.* **1998**, *286*, 253.
38. Frisch, M. J.; Trucks, G. W.; Schlegel, H. B.; Scuseria, G. E.; Robb, M. A.; Cheeseman, J. R.; Montgomery, J. A., Jr.; Vreven, T.; Kudin, K. N.; Burant, J. C.; Millam, J. M.; Iyengar, S. S.; Tomasi, J.; Barone, V.; Mennucci, B.; Cossi, M.; Scalmani, G.; Rega, N.; Petersson, G. A.; Nakatsuji, H.; Hada, M.; Ehara, M.; Toyota, K.; Fukuda, R.; Hasegawa, J.; Ishida, M.; Nakajima, T.; Honda, Y.; Kitao, O.; Nakai, H.; Klene, M.; Li, X.; Knox, J. E.; Hratchian, H. P.; Cross, J. B.; Adamo, C.; Jaramillo, J.; Gomperts, R.; Stratmann, R. E.; Yazyev, O.; Austin, A. J.; Cammi, R.; Pomelli, C.; Ochterski, J. W.; Ayala, P. Y.; Morokuma, K.; Voth, G. A.; Salvador, P.; Dannenberg, J. J.; Zakrzewski, V. G.; Dapprich, S.; Daniels, A. D.; Strain, M. C.; Farkas, O.; Malick, D. K.; Rabuck, A. D.; Raghavachari, K.; Foresman, J. B.; Ortiz, J. V.; Cui, Q.; Baboul, A. G.; Clifford, S.; Cioslowski, J.; Stefanov, B. B.; Liu, G.; Liashenko, A.; Piskorz, P.; Komaromi, I.; Martin, R. L.; Fox, D. J.; Keith, T.; Al-Laham, M. A.; Peng, C. Y.; Nanayakkara, A.; Challacombe, M.; Gill, P. M. W.; Johnson, B.; Chen, W.; Wong, M. W.; Gonzalez, C.; Pople, J. A. Gaussian 03, Revision A.1 Gaussian, Inc., Pittsburgh PA, **2003**.
39. Nair, B. R.; Francis, D. J. *Polymer* **1983**, *24*, 626.